Diastereoselective Attack on Chiral-at-Metal Ruthenium Allenylidene Complexes to Give Alkynyl Complexes

Matthew J. Queensen,[a] Nigam P. Rath,[a,b] Eike B. Bauer*[a]

[a] University of Missouri - St. Louis, Department of Chemistry and Biochemistry, One University Boulevard, St. Louis, MO 63121, USA. Tel.: +1-314-516- 5311; Fax: +1-314-516-5342. bauere@umsl.edu

[b] Center for Nanoscience, University of Missouri - St. Louis, St. Louis, MO, 63121, USA.

Supporting Information

1. Experimental and spectroscopic data for the generation of the enynyl complex (R_{Ru},R_{ax})-**13**

The reaction between (*R*$_{Ru}$,*R*$_{ax}$)-**12** and 1-phenylethenolate did not result in a nucleophilic attack at the C_γ atom, but resulted mainly in deprotonation of the methyl group to give the neutral eneynyl complex (*R*$_{Ru}$,*R*$_{ax}$)-**13** (Scheme S1).

Scheme S1. Enynyl formation.

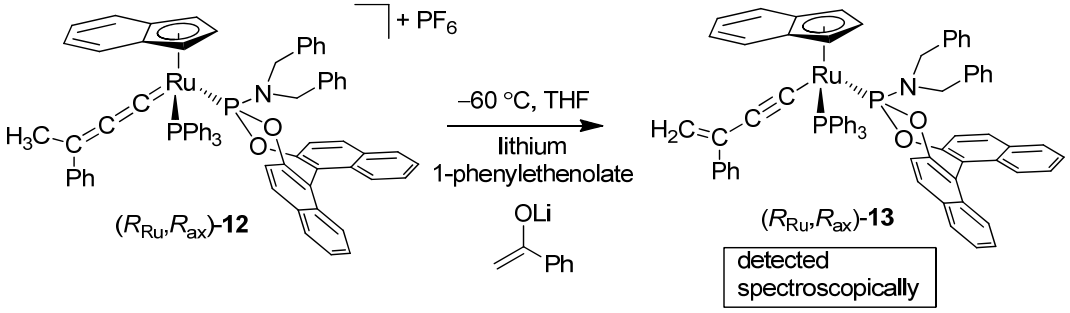

The complex could not be isolated spectroscopically pure; the isolated material contained other, unidentified material. However, key NMR and IR data in addition to the FAB-MS of the crude material established the formation of (*R*$_{Ru}$,*R*$_{ax}$)-**13**. The terminal =C*H*$_2$ unit gave two signals at 5.29 and 4.93 ppm in the ^{1}H NMR and a diagnostic signal at 110.2 ppm in the ^{13}C{^{1}H} NMR in addition to signals at 113.6 and 112.1 ppm for the Ru-*C*≡*C* carbon atoms. Also, bands at 2069 cm^{-1} and 2034 cm^{-1} were observed in the IR, while the band around 1950 cm^{-1} diagnostic for allenylidene complexes has disappeared. These spectroscopic data closely resemble those of previously synthesized enynyl complexes. It has previously been reported that hydrogens on carbon atoms in a position alpha to the C_γ atom of the allenylidene chain can be considerably acidic. Such protons can be removed by bases as weak as K_2CO_3, as shown for an allenylidene

complex $[Ru(Ind)(PPh_3)_2{=}C{=}C{=}C(CH_2)R]^+$ which gave upon deprotonation a enynyl complex (R denotes a cyclic steroid backbone, of which the CH_2 group is a member).

Generation of (R_{Ru},R_{ax})-[Ru(Ind)(PPh_3)(6){C≡C–C=(CH_2)Ph}]$^+$ PF_6^- [(R_{Ru},R_{ax})-13]. A two neck round bottom flask was charged with acetophenone (0.277 g, 2.31 mmol) and THF (2 mL). The flask was then cooled to –60 °C followed by the rapid addition of freshly titrated LDA (5 mL, 0.46 M) and the solution was stirred at –60 °C for two hours and then warmed to room temperature. To a separate Schlenk tube was added (R_{Ru},R_{ax})-[Ru(Ind)(PPh_3)(**6**){=C=C=C(CH_3)Ph}]$^+$ PF_6^- (0.232 g, 0.228 mmol) and THF (10 mL) and the solution was cooled to –60 °C for 10 minutes followed by the dropwise addition of the prepared acetophenone enolate (0.801 mL, 0.329 M, 0.341 mmol) over the course of 7 minutes. The solution was stirred at –60 °C for 2 hours and at room temperature for 2 hours. The solvent was removed by oil pump vacuum to yield the crude solid as a mixture of alkynyl-vinylidene and enolate attack products. The crude solid was purified by flash column chromatography (2 × 30 cm silica column, eluted with 2:1 v/v CH_2Cl_2/diethyl ether) to yield (**R_{Ru},R_{ax})-13** as impure orange solid (0.129 g, 0.094 mmol, 42 %). Key NMR assignment data (δ, $CDCl_3$): ^{1}H 5.29 (s, 1H, C=C*H)*, 4.93 (s, 1H, C=C*H)*. $^{13}C\{^1H\}$: 113.6 (s, C_α), 112.1 (s, C_β), 110.2 (s, PhC=CH_2). $^{31}P\{^1H\}$: 177.98 (d, $^3J_{PP}$=124.7 Hz, (*R*)-**6**), 55.55 (d, $^3J_{PP}$=123.9 Hz, PPh_3). IR (cm^{-1}, ATR): 3428(m), 3056(w), 2069(s), 2034(s), 1683(m), 1590(m), 1464(s), 1433(s), 1325(s), 1229(s), 1092(s), 952(s), 822(s), 743(s), 693(s). MS (FAB): 1116 ([(**R_{Ru},R_{ax})-13**]$^+$, 35%), 988 ([(**R_{Ru},R_{ax})-13** –C≡C-PhC=CH_2]$^+$, 10%), 854 ([(**R_{Ru},R_{ax})-13** – PPh_3]$^+$, 60%).

2. Table S1 (Crystallographic Parameters)

	$[(R_{Ru},R_{ax})$-**11**$]^{+}PF_6^{-}$ $\cdot CH_2Cl_2$	(R_{Ru},R_{ax})-**17**·toluene
Empirical formula	$C_{79}H_{66}Cl_2F_6NO_2P_3Ru$	$C_{91}H_{73}NO_3P_2Ru$
Formula weight	1440.20	1391.51
Temperature	100(2) K	100(2) K
Wavelength	0.71073 Å	0.71073 Å
Crystal system	Triclinic	Orthorhombic
Space group	P1	$P2_12_12_1$
Unit cell dimensions a, b, c [Å]	a = 11.1558(9) Å b = 11.8706(8) Å c = 14.5713(11) Å	a = 14.1888(4) Å b = 17.6625(5) Å c = 29.0539(9) Å
Unit cell dimensions α, β, γ [deg]	α= 110.713(4)° β= 96.502(4)° γ = 107.918(4)°	α= 90° β= 90° γ = 90°
Volume / Z	1663.0(2) $Å^3$ / 1	7281.2(4) $Å^3$ / 4
Density (calculated)	1.438 Mg/m^3	1.269 Mg/m^3
Absorption coefficient	0.455 mm^{-1}	0.311 mm^{-1}
F(000)	740	2896
Crystal size / mm^3	0.219 × 0.187 × 0.059	0.432 × 0.174 × 0.079
Theta range for data collection	1.945 to 28.356°	1.597 to 27.117°
Index ranges	$-14 \le h \le 14$, $-15 \le k \le 15$, $-19 \le l \le 19$	$-18 \le h \le 18$, $-14 \le k \le 22$, $-37 \le l \le 37$
Reflections collected	38508	148862
Independent reflections	15431 [R(int) = 0.0424]	16056 [R(int) = 0.0715]
Completeness to theta = 25.242°	99.9 %	99.8 %
Absorption correction	Semi-empirical from equivalents	Semi-empirical from equivalents
Max. and min. transmission	0.8621 and 0.7834	0.9281 and 0.8579
Refinement method	Full-matrix least-squares on F^2	Full-matrix least-squares on F^2
Data / restraints / parameters	15431 / 589 / 798	16056 / 140 / 822
Goodness-of-fit on F2	1.024	1.050
Final R indices [I>2sigma(I)]	R1 = 0.0477, wR2 = 0.1098	R1 = 0.0438, wR2 = 0.1142
R indices (all data)	R1 = 0.0550, wR2 = 0.1149	R1 = 0.0545, wR2 = 0.1222
Absolute structure parameter	–0.032(11)	–0.010(8)
Extinction coefficient	n/a	n/a
Largest diff. peak and hole	0.726 and –0.769 e.$Å^{-3}$	0.964 and –0.416 e.$Å^{-3}$

3. UV-vis spectra of selected complexes

(R_{Ru},R_{ax})-**11** (blue)

(R_{Ru},R_{ax})-**18** (orange)

(R_{Ru},R_{ax})-**19** (yellow)

(R_{Ru},R_{ax})-**20** (grey)

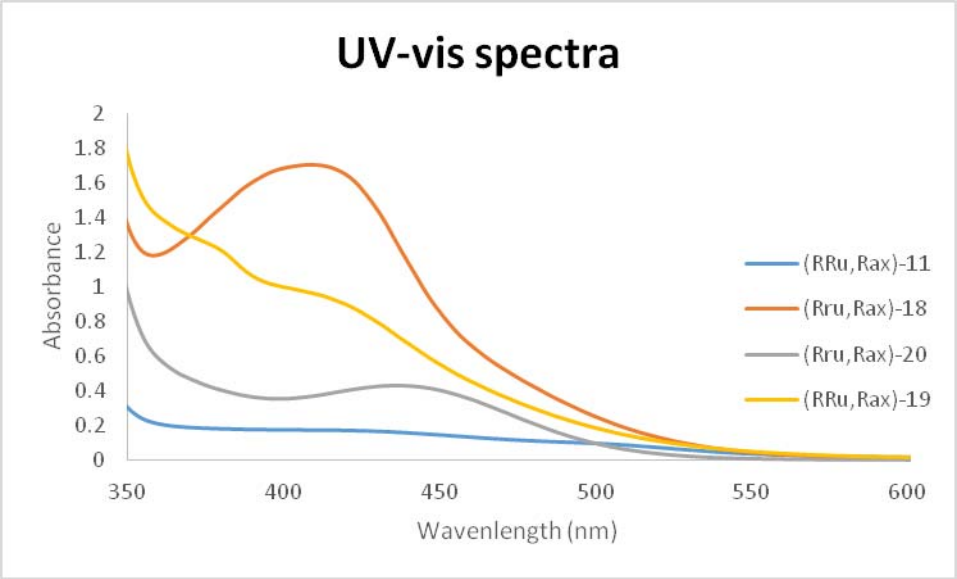

4. $^{31}P\{^{1}H\}$ NMR complexes for the determination of diastereomeric excesses

Integration of the $^{31}P\{^{1}H\}$ NMR spectra of (R_{Ru},R_{ax})-**18** (top) and (R_{Ru},R_{ax})-**20** (bottom) for the determination of enantiomeric excesses.

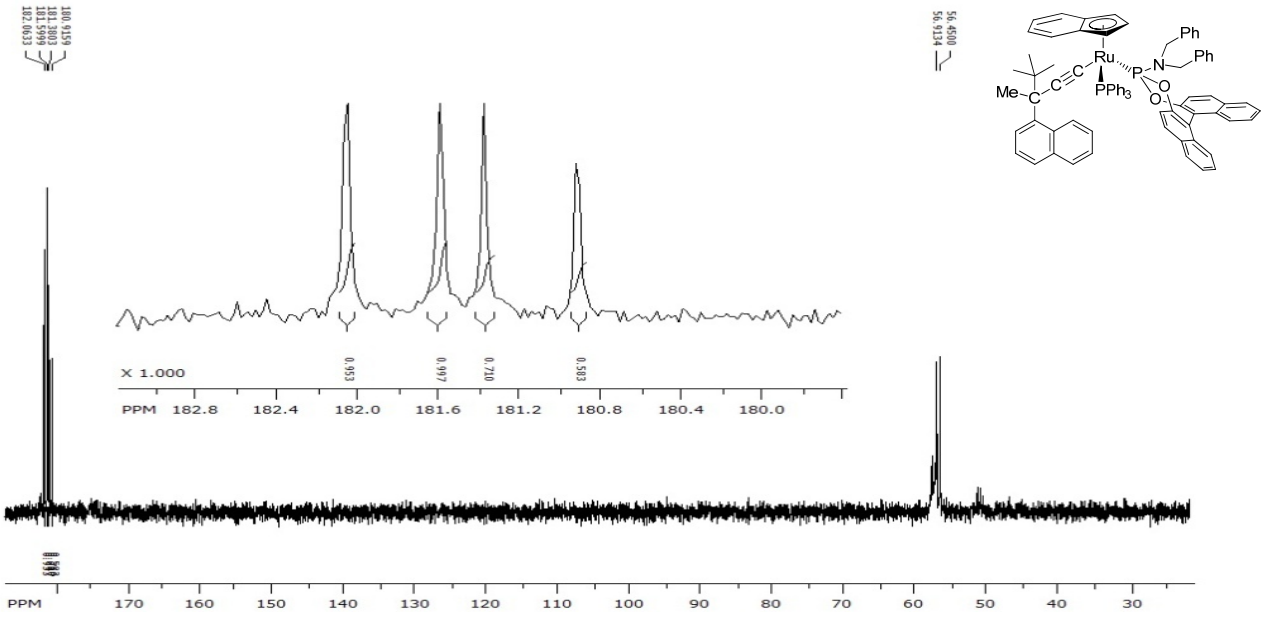

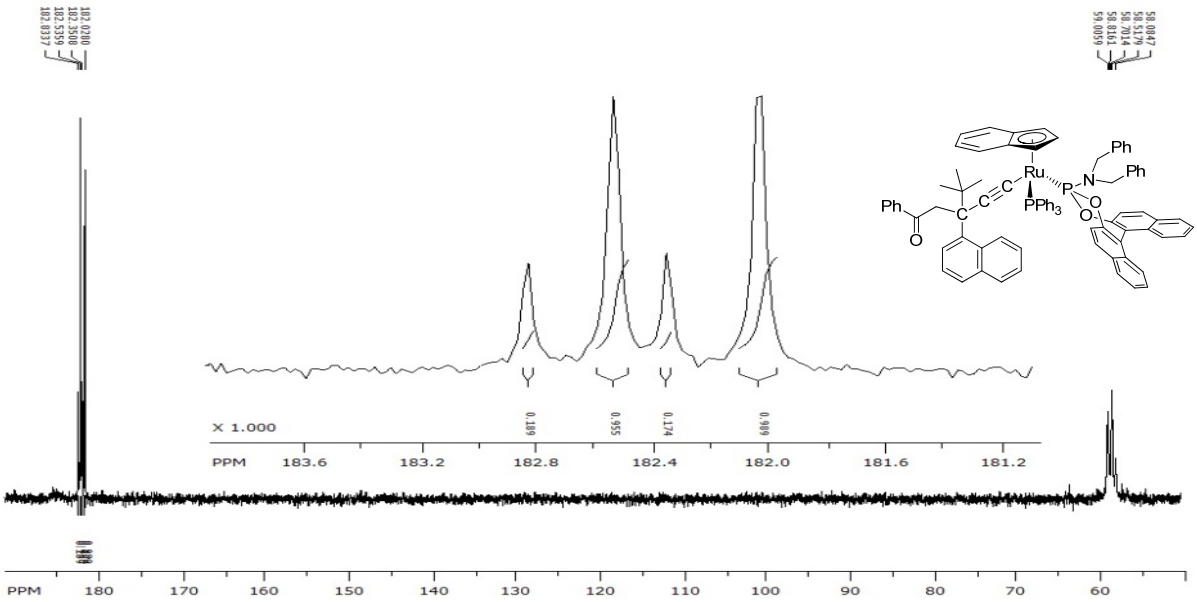

^{1}H and ^{13}C{^{1}H} NMR spectra of (R_{Ru},R_{ax})-[Ru(Ind)(PPh$_3$)(**6**){=C=C=C(*t*-Bu)(2-napthyl)}]$^{+}$PF$_6^{-}$, [(R_{Ru},R_{ax})-**11**]

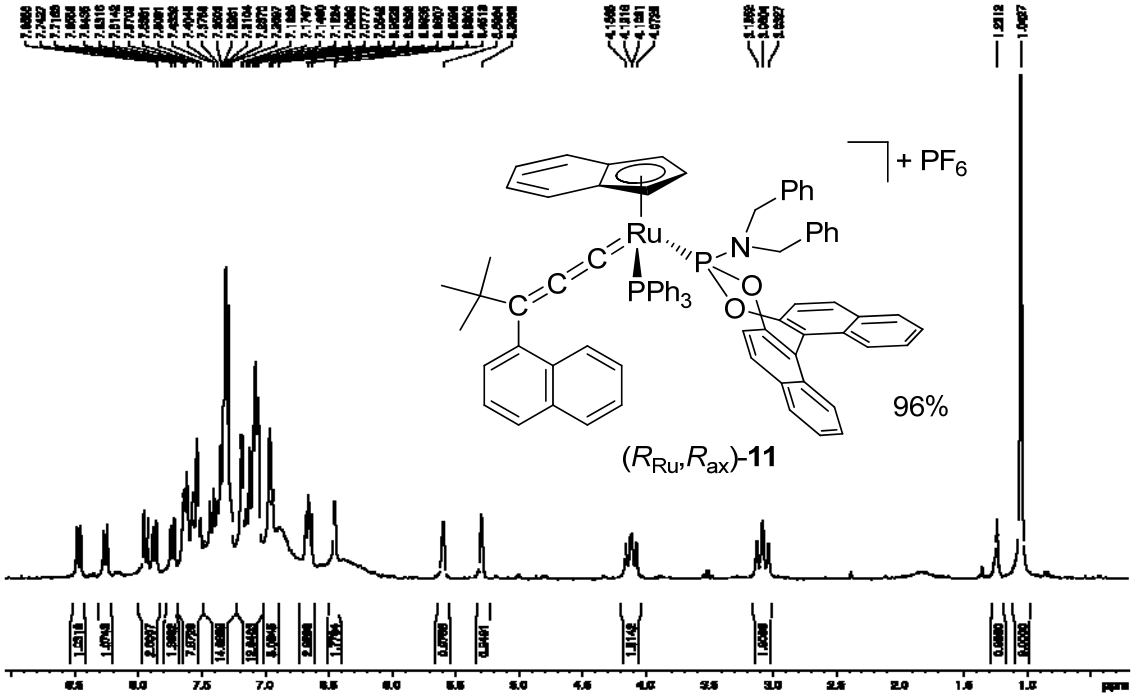

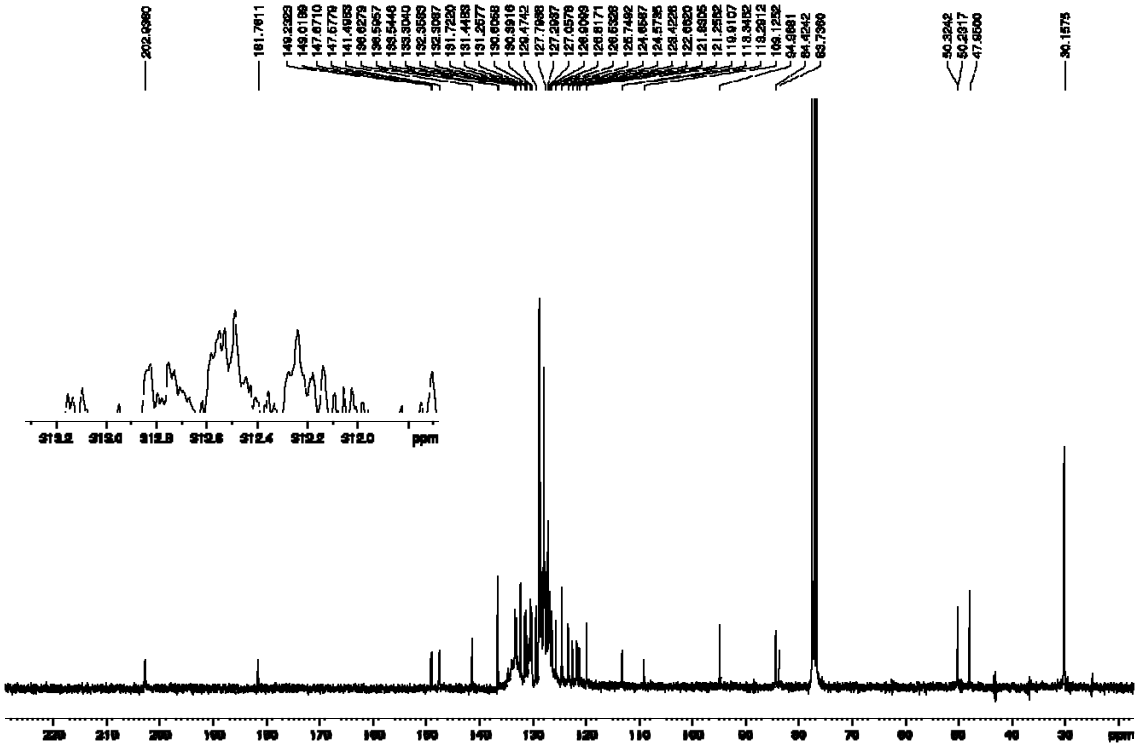

^{1}H and ^{13}C{^{1}H} NMR spectra of (R_{Ru},R_{ax})-[RuCl(Ind)(PPh$_3$)(**6**)(C≡C–CPh$_2$Me)], [(R_{Ru},R_{ax})-**14**]

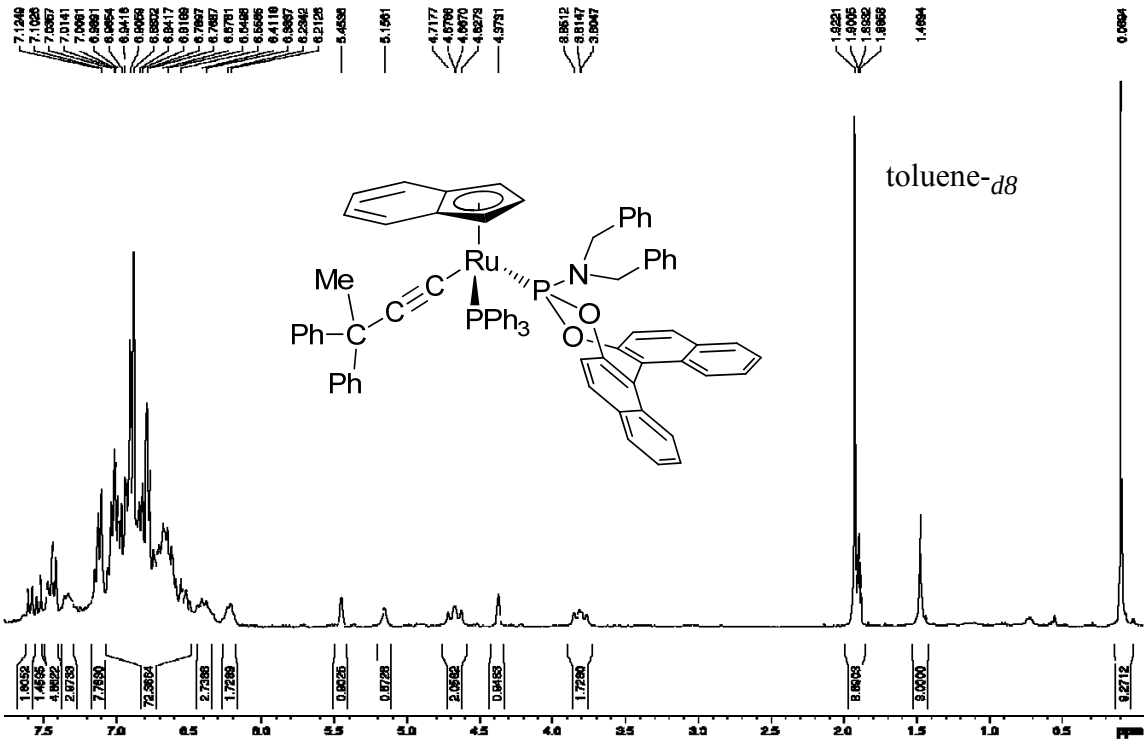

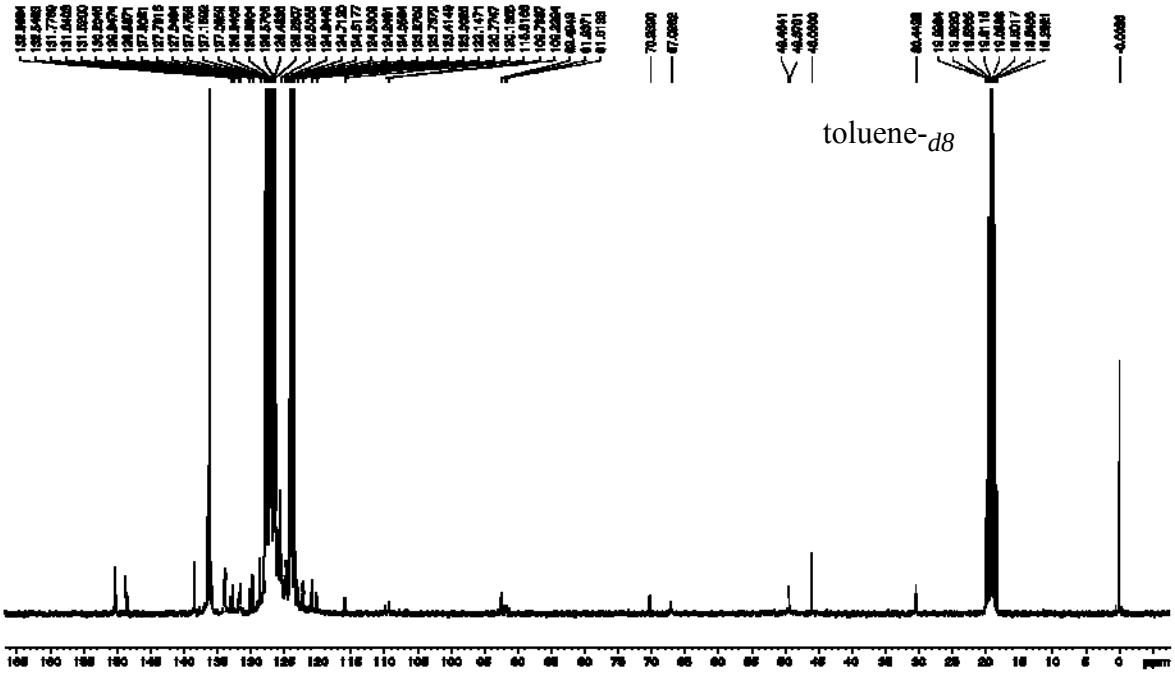

(R_{Ru},R_{ax})-[RuCl(Ind)(PPh_3)(**6**)(C≡C–CPh_2*n*-Bu)], [(R_{Ru},R_{ax})-**15**]

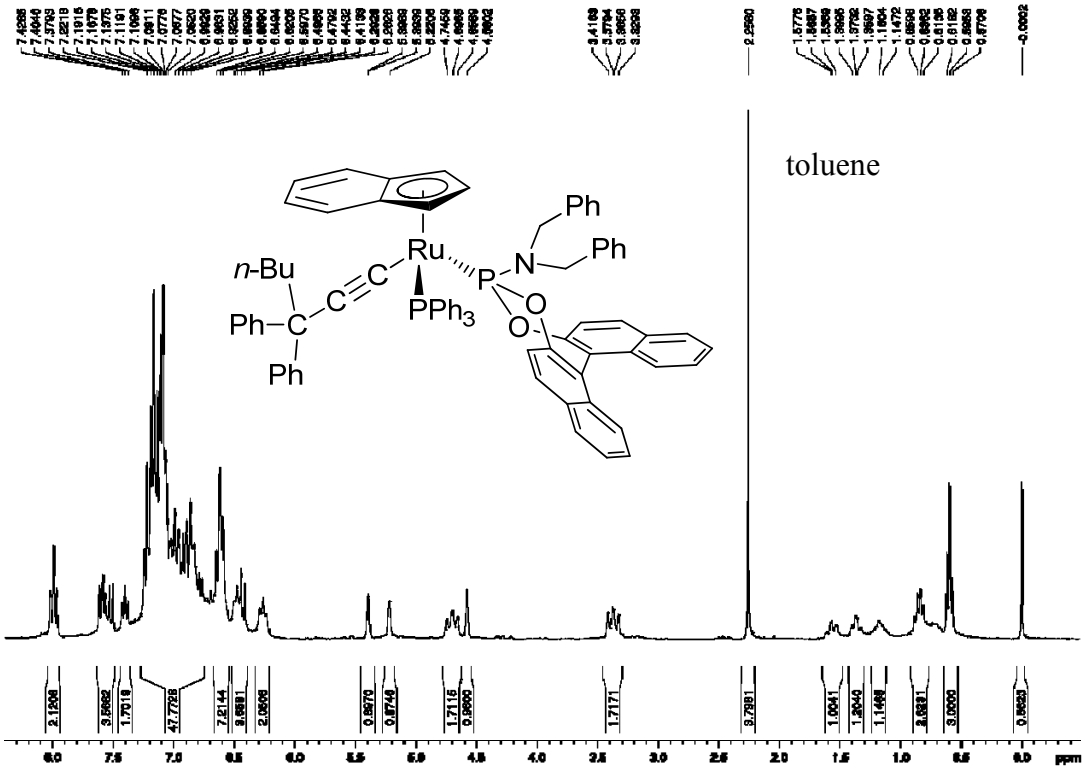

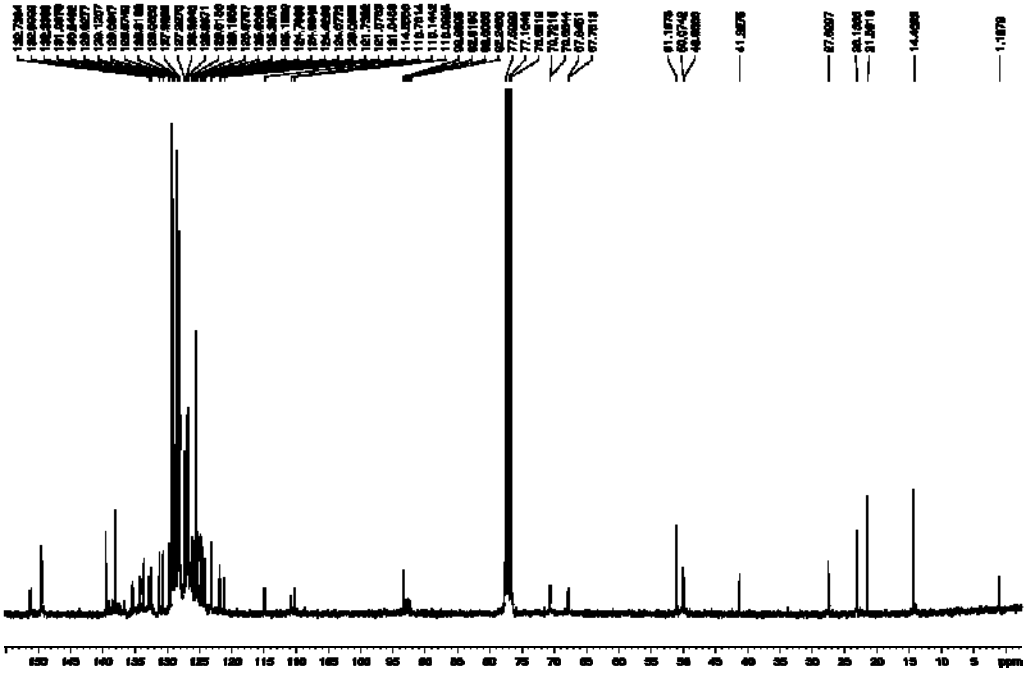

(R_{Ru},R_{ax})-[RuCl(Ind)(PPh_3)(**6**)(C≡C–CPh_2C≡CPh)], [(R_{Ru},R_{ax})-**16**]

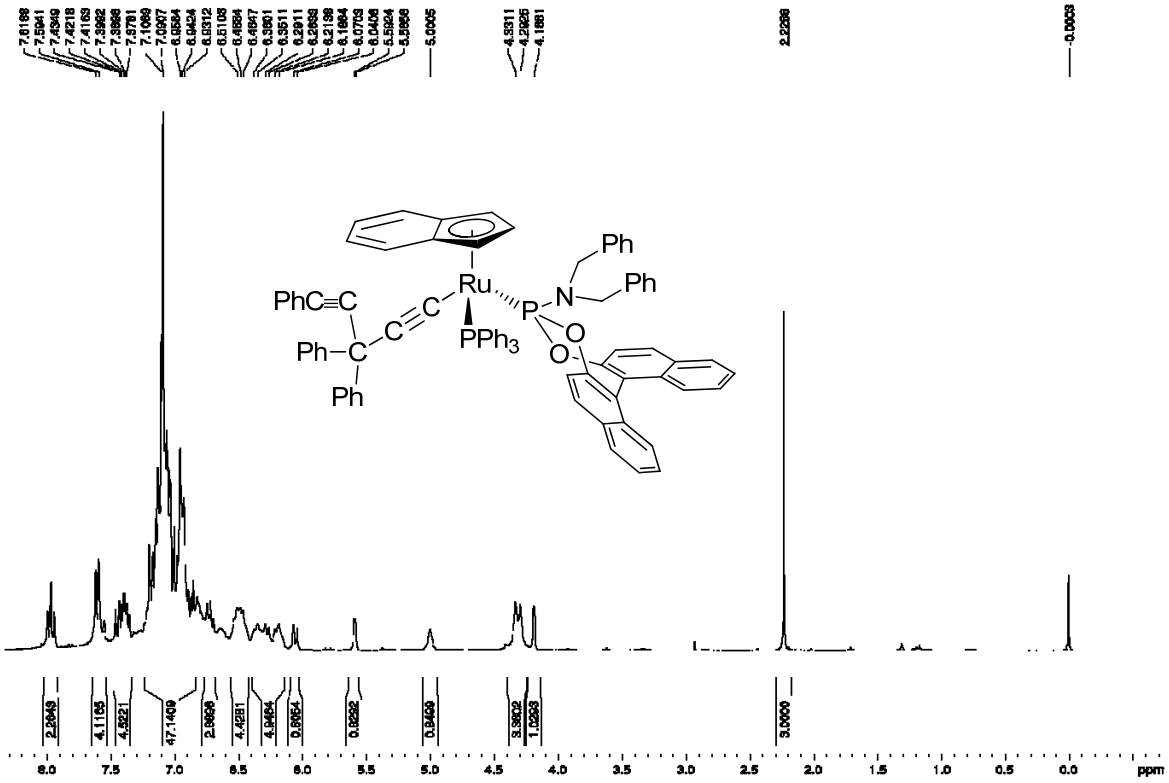

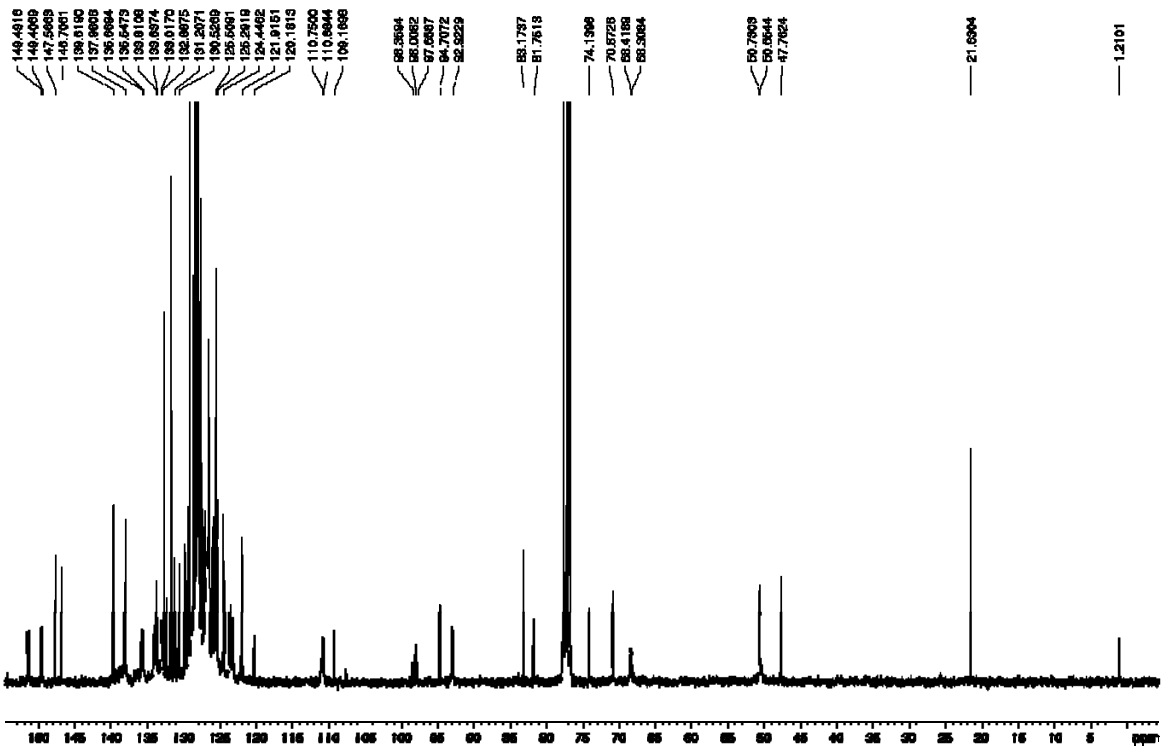

(R_{Ru},R_{ax})-[RuCl(Ind)(PPh_3)(**6**){C≡C–$CPh_2CH_2C(O)Ph$}], [(R_{Ru},R_{ax})-**17**]

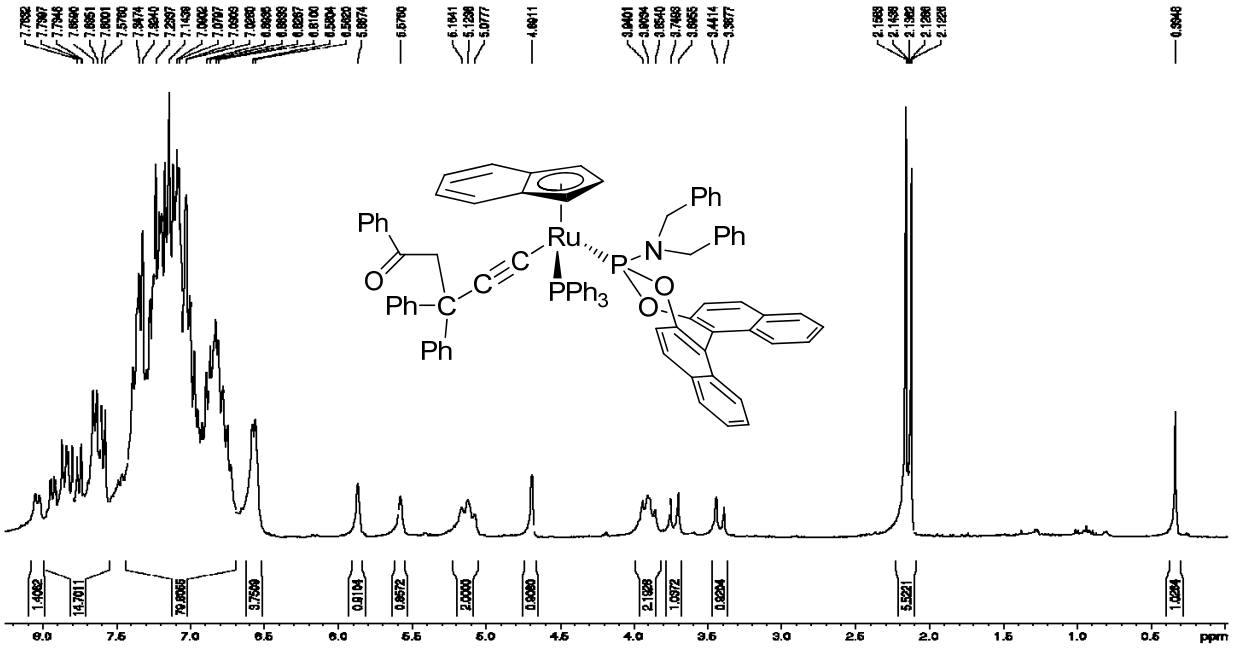

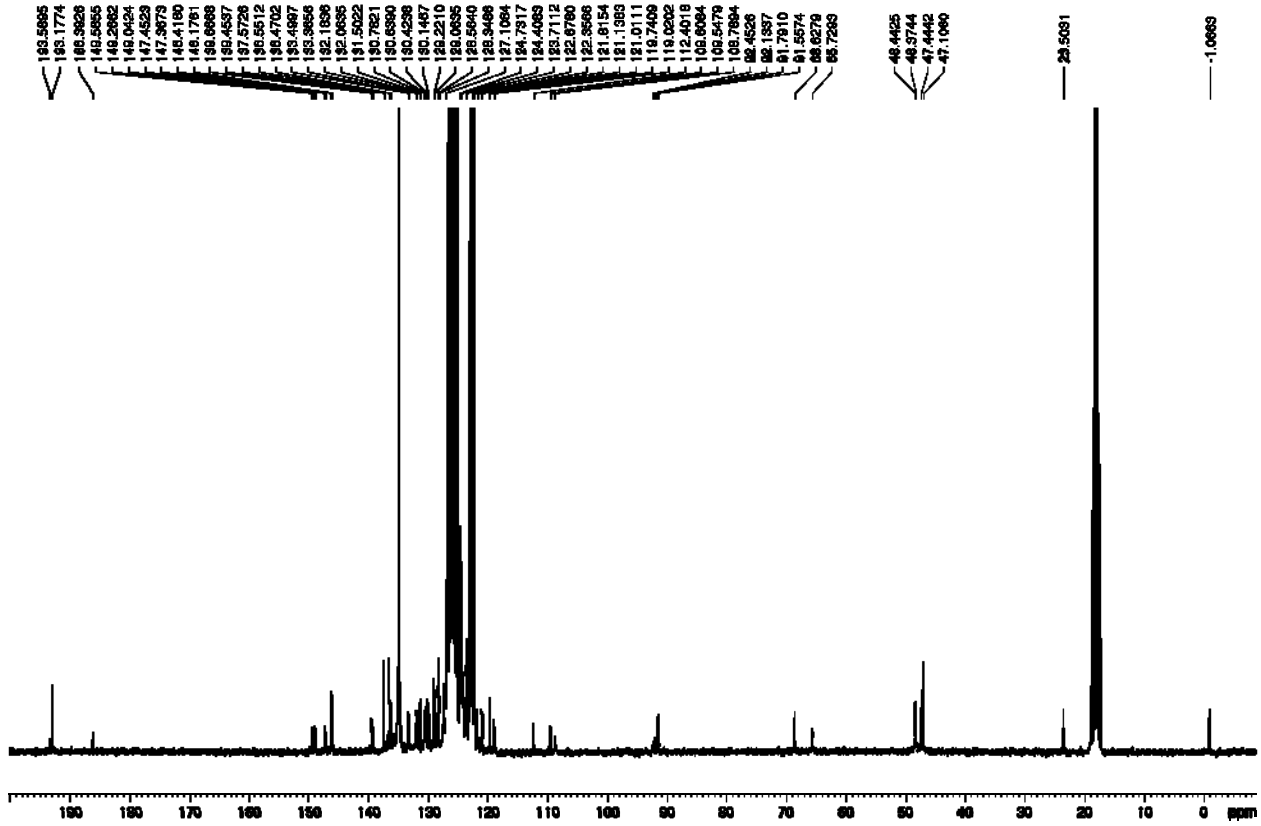

(R_{Ru},R_{ax})-[Ru(Ind)(PPh_3)(**6**){C≡C–C(*t*-Bu)(2-napthyl)CH_3}], [(R_{Ru},R_{ax})-**18**]

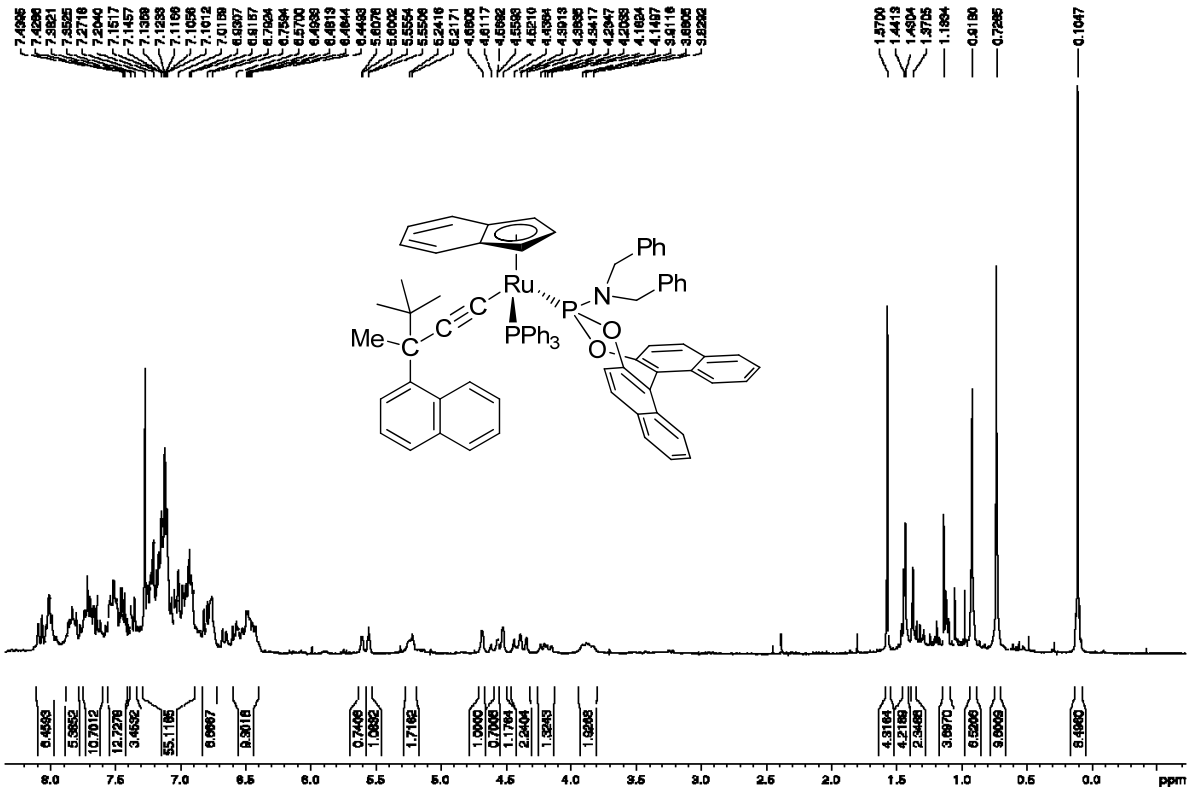

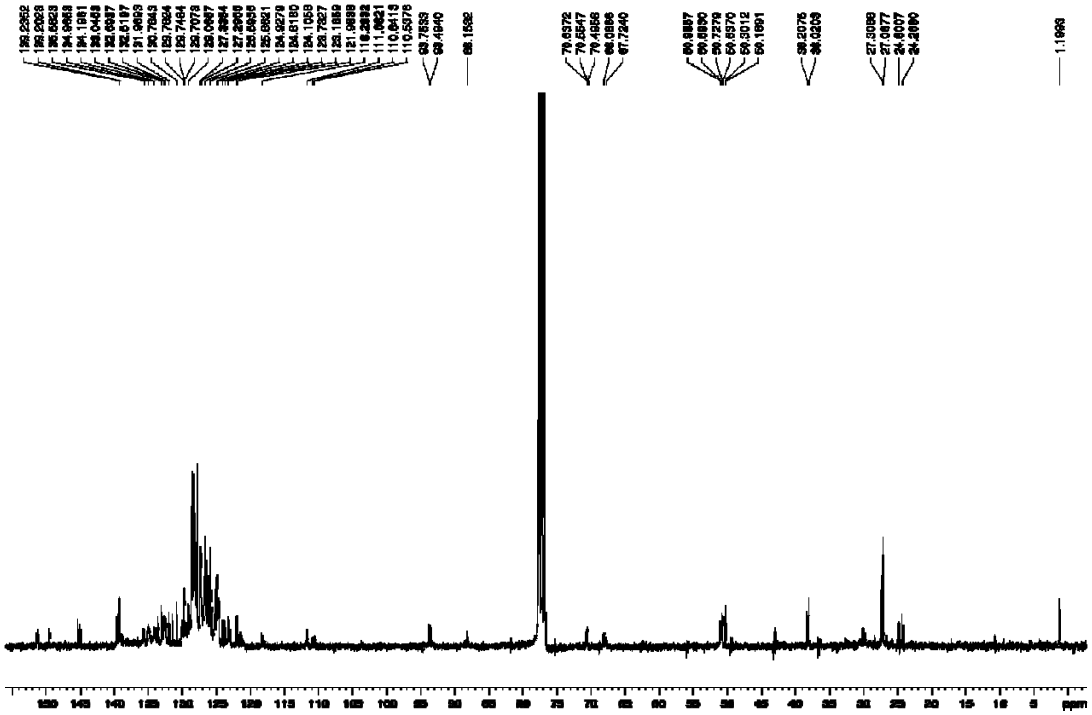

(R_{Ru},R_{ax})-[Ru(Ind)(PPh_3)(**6**){C≡C–C(*t*-Bu)(2-napthyl)C≡CPh}], [(R_{Ru},R_{ax})-**19**]

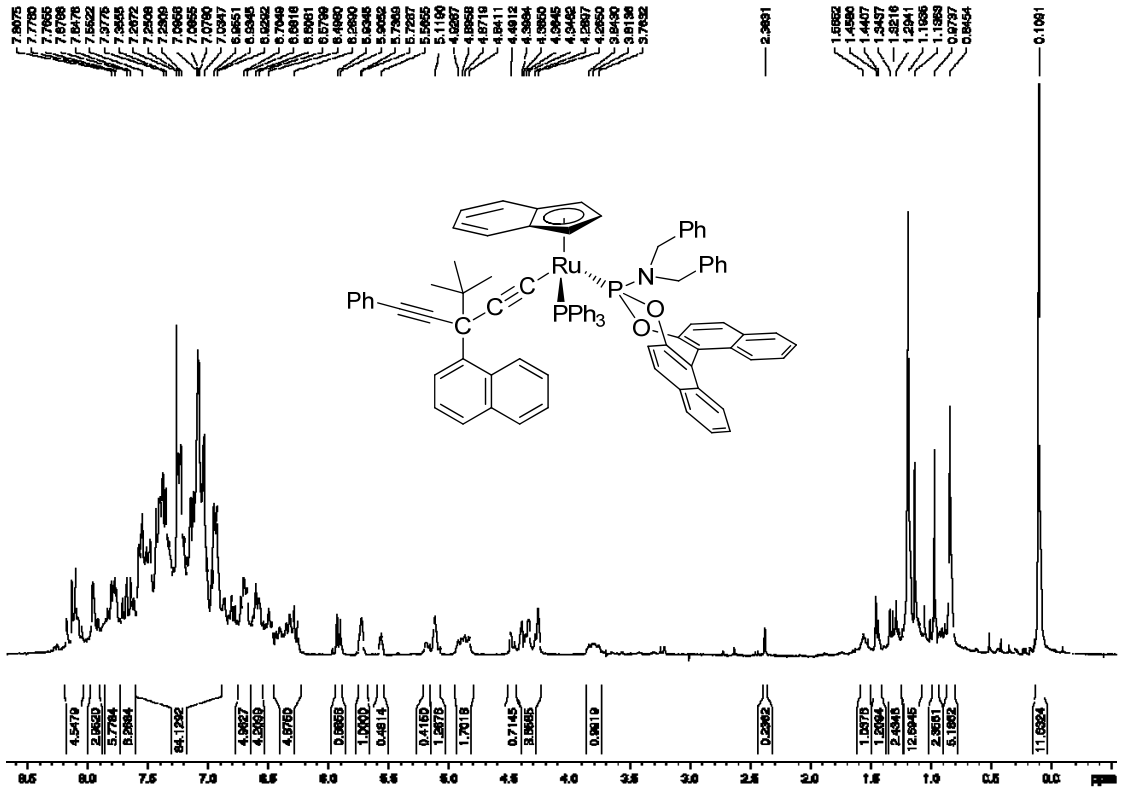

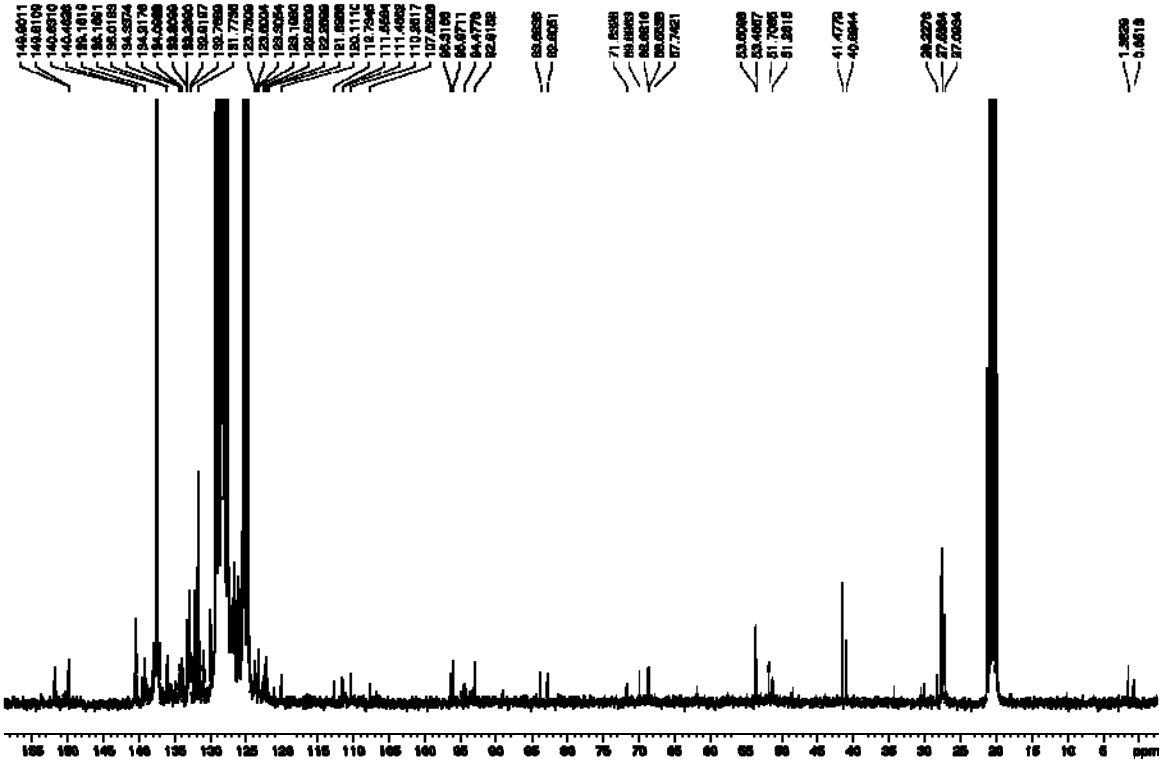

(R_{Ru},R_{ax})-[Ru(Ind)(PPh_3)(**6**){C≡C–C(*t*-Bu)(2-napthyl)CH_2C(O)Ph}], [(R_{Ru},R_{ax})-**20**]